

PHOTOCATALYTIC DEGRADATION OF ACID BLUE 25 DYE IN WASTEWATER
BY ZINC OXIDE NANOPARTICLESEmmanuel Amuntse Yerima¹, Edwin Ogwuche², Chijindu Ifeanyi Ndubueze², Khairat Asabe Muhammed²,
James Dama Habila^{1,2*}¹Department of Chemical Sciences, Faculty of Pure and Applied Sciences, Federal University Wukari, PMB 1020, Wukari, Nigeria²Department of Chemistry, Faculty of Physical Sciences, Ahmadu Bello University, PMB 1045, Zaria, Nigeria

*Corresponding email: yerimaemmanuel@yahoo.com

Received: 26.02.2024; **Accepted:** 28.03.2024; **Available online:** 30.03.2024 **Published:** 30.03.2024**Cite this article:** Yerima, E. A., Ogwuche, E., Ndubueze, C. I., Muhammed, K. A., & Habila, J. D. (2024). Photocatalytic Degradation of Acid Blue 25 Dye in Wastewater by Zinc Oxide Nanoparticles. *Trends in Ecological and Indoor Environment Engineering*, 2(1), 50–55.

This study investigates the photocatalytic degradation of Acid Blue Dye using zinc oxide nanoparticles synthesized from *Senna siamea* flower extracts (ZnO-S.S.). The synthesized nanoparticles were investigated using Transmission Emission Spectroscopy (TEM) and Scanning Electron Microscope (SEM), which made it possible to reveal the spherical shape of ZnO-S.S. nanoparticles. Thermogravimetric Analysis – Differential Thermal Analysis (TGA-DTA) revealed high thermal stability of ZnO-S.S. with an insignificant weight loss as temperature increases from 600 °C to 846.9 °C. While Energy Dispersive X-ray analysis (EDX) reveals the elemental composition and atomic weight percentage as C (4.8%), O (11%), S (6%) and Zn (78.2%). The synthesized nanoparticles ZnO-S.S. used to degrade Acid Blue dye contaminated waste water under visible light irradiation. Exhibits an optimum degradation efficiency of 99% achieved in 150 minutes using a catalyst dosage of 150 mg at an initial acid blue concentration of 10 mg/L. The degradation process best conformed to the pseudo first order kinetics pathway. In conclusion the study established that the synthesized catalyst exhibits good efficiency and utility in degrading dye contaminated wastewater. However, further studies are recommended on the influence of other indicators such as light intensity, temperature and pH on the degradation process.

Keywords: wastewater; Acid Blue Dye; visible light; degradation efficiency; kinetics; energy dispersive X-ray analysis.

INTRODUCTION

The wide range of contaminants present in the environment is as a result of excessive demands on society due population growth, urbanization and industrialization (Inyinbor et al., 2018). Thus, the excellent of water at once influences the lifestyles general of people and animals. The major water means of contaminating water are from commercial discharge of chemicals, agricultural movements, sewage drains and different environmental changes (Yerima et al., 2022).

Water pollution might also exist in one of these kinds like pharmaceutical wastes, pesticides, herbicides, fabric dyes, resins, and phenolic compounds (Zhang & Fang, 2010). Out of which approximately 10–15% of dyes such as acid blue among others are launched into the surroundings at some stage in dyeing manner making the effluent exceptionally coloured and aesthetically unpleasant. The effluent from fabric industries as a result contains a massive range of dyes and different components that are introduced for the duration of the colouring process (Wang et al., 2002). Traditional methods are unable to remove them from contaminated waters, and due to the high solubility of dyes in water, there is an opportunity for their widespread distribution through sewers and rivers. What's even worse is that such substances can decompose to form highly toxic and carcinogenic products (Rindle et al., 1975). Even, small quantities of waste water effluents might also exert unfavourable fitness consequences on people and the ecosystems. Hence, commercial discharge of wastewater calls for right sewage remedy for sustainable wastewater management (Donkadokula et al., 2009).

Wastewater remediation technologies have provided numerous green methods of waste water management; however excessive cost and time are needed in putting them to effect (Gupta et al., 2012). Recently, semiconductor

photocatalysis emerges to be a promising technique with the capability of effecting degradation of diverse organic pollutants in wastewater when sunlight or UV-visible light is use as a source of irradiation (Ansari et al., 2015; Ahmed et al., 2017).

Green-synthesized metallic nano-particles play significant roles in nanotechnology spanning diverse fields (Awwad et al., 2015; Kpega et al., 2023). For instance, ZnO nanoparticles have been employed as an adsorbent due to their low toxicity and efficiency as adsorbent (Azizi et al., 2017). While the plant-based synthesized ZnO nanoparticles enhances metal ion adsorption capacity due to the chemical interactions between ions and functional groups of plant extracts. Previous studies have reported the use of *Passiflora foetida* extracts-ZnO nanoparticles to efficiently degrade both methylene blue (MB) and Rhodamine blue (RhB) dyes with nearly 93.25% and 91.06% efficiency in 70 minutes (Khan et al., 2021). Likewise, Congo Red dye have been degraded successfully using zinc oxide nanoparticles.

Green-synthesized metallic nano-particles can be produced by biological methods and provides an environmentally friendly way of synthesizing nano-particles devoid of harmful and toxic chemicals (Singh, 2016; Agarwal et al., 2018).

The current study purpose is to investigate the photocatalytic activity of zinc oxide nanoparticles synthesized from *Senna siamea* flower extracts. Zinc oxide nanoparticles were synthesized through green synthesis using *Senna siamea* flower extract. The main outcome of the study is expected to achieve the degradation of Acid Blue Dye in synthetic wastewater by studying the effect of concentration, dosage and time using a simple photo reactor with the hope of providing a sustainable and eco-friendly means of acid blue wastewater treatment. Acid Blue Dye is an acid dye that is water-soluble, the second largest class of textile dyes extensively used in the industries due to their wide array of colour shades with the IUPAC name sodium 1-amino-4-anilino-9,10-dioxanthracene-

2-sulfonate with the chemical formula of (C₂₀H₁₃N₂NaO₅S) (Figure 1).

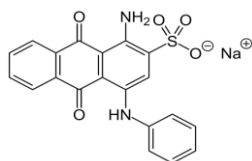


Figure 1. Molecular Structure of Acid Blue 25 Dye

Because these substances have a fused aromatic structure that persists for a long time, they are highly resistant to degradation and accumulation in soil and wastewater. As a result, there is a need to search for methods that prevent environmental pollution by these toxic substances (Moulin, 2014).

MATERIALS AND METHODS

Chemical substances used

All the reagents used in this work were of analytical grade and were used without any further purification: zinc nitrate (Zn(NO₃)₂·6H₂O, 297.49 g, 99.0%, Sigma – Aldrich) Sodium Hydroxide (NaOH, Sigma – Aldrich, 40 g) Hydrochloric acid (Sigma – Aldrich, 37% w/v) and Acid Blue 25 Dye (Kem Light Laboratories Pvt. Ltd., 416.4 g).

Sample Collection, Identification and Preparation

Senna siamea flowers were collected in the morning within the Faculty of Physical Sciences, and were identified at the Herbarium, Department of Biological Sciences, Ahmadu Bello University, Zaria (Figure 2). The flowers were cleaned by washing several times with running water and subsequently with distilled water. The flowers were dried for 12 days at room temperature, without direct sunlight, until all moisture was completely lost. A coarse powder was obtained from dried flowers by grinding, 5 g of which were boiled in 50 cm³ of double distilled water for 15 minutes. The cooled aqueous extract was filtered through Whatman No. 1 filter paper and stored in a refrigerator at 4 °C to remain suitable for experimental study.



Figure 2. Image of *Sienna siamea* flower (<https://tropical.ferns.info/query.php>)

Zinc oxide nanoparticles

To 50 mL of the *Sienna siamea* extract was added in a conical flask, 5 g of zinc oxide was added to the solution. After reaction, mixture was further stirred by means of magnetic stirrer for 3 hours at 70 °C for even stirring. Then, the reaction mixtures were centrifuged at 4000 rpm for 10 minutes; the solid product suggesting the presence of ZnO-NPs (Jayachandran et al., 2021; Kpega et al., 2023). The solid products were then rinsed with distilled water and developed by heating at 450 °C over a period of 3 hours in a hot air oven. The catalyst synthesized was coded as ZnO-S.S.

Characterization of Synthesized Zinc oxide Nanoparticles

Transmission Emission Spectroscopy (TEM)

A NanoMill Transmission Emission Microscope operated at 20 kV was used to examine the internal structure of

synthesized catalyst. Approximately 0.02 g of the sample was dissolved in 10 cm³ of ethanol, followed by ultra-sonication for 5 minutes. A drop of the solution was placed on a holey-carbon copper grid and air dried at room temperature and thereafter exposed to photo light for 3 minutes. After drying, the copper grids with sample were mounted into the electron microscope for analysis.

Thermo Gravimetric Analysis (TGA)

TGA was employed to investigate the thermal and energy profile of the synthesized catalyst. A Perkin-Elmer TGA 400 device that is efficient at heating rate of 10 °C per minute in nitrogen (N₂) atmosphere was employed in determining the thermal characteristics of the catalyst. The sample was heated up to 950 °C. Thermal Analysis detects the interatomic and inter- or intramolecular interactions as related to an imposed external change in temperature. The nitrogen gas was set as the inert gas and oxygen gas as the oxidative. The gas environment was preselected for thermal decomposition (inert-nitrogen gas) and an oxidative decomposition (air or oxygen). The required flow rate was adjusted to provide the appropriate environment for the tests. The samples were then placed in the specimen holder and the temperature of the furnace was raised to 950 °C. The initial weight was set to read 100% before the heating program was initiated.

Scanning Electron Microscopy (SEM)

To visualize the size and surface morphology of the sample after modification, Scanning Electron Microscopy (SEM) was carried out using JEOL-JSM 7600F Scanning Electron Microscope of the Department of Geology, University of Ibadan, Ibadan. Mandatory sample preparation involves creating it, placing the sample on a clean carbon strap so as to ensure its visibility through the SEM chamber. Measures are also required to prevent charge accumulation and prevent contact of the sample with the detector.

Energy Dispersive X-ray (EDX) Analysis

Approximately 0.05 mg of the catalyst was sprinkled on a sample holder covered with carbon adhesive tape for 5 minutes prior to analysis. The sample was characterized using the JEOL-JSM 7600F Scanning Electron Microscope equipped with EDX. The secondary electron mode was activated for imaging and a homogeneous region on the sample was identified. The microscope was operated with electron high tension of 20 kV for EDX. The illumination angle was adjusted to 150° and then the elemental composition of the sample was determined.

Preparation of Reagents and Stock Solution

Preparation of acid blue stock solution

Acid Blue dye (0.5 g) was dissolved in a 1000 mL volumetric flask and made to the mark with deionized water to obtain 500 mg/L stock solution. Working concentrations of between 5 mg/L, 10 mg/L and 15 mg/L were prepared separately from the stock solution.

Preparation of Acid Blue calibration standards

Calibration standards of the following concentrations were prepared from the stock solution: 2, 4, 6, 8 and 10 mg/L. Their absorbance were measured at a maximum wavelength of 674 nm using distilled water as blank and a calibration curve of absorbance against concentration was plotted to obey Beer Lambert's law. An equation of straight line was generated in order to determine residual concentration of dye left for subsequent spectrophotometric analysis of the dye degradation.

Photocatalytic Degradation Experiment

The Photocatalytic activity was evaluated by batch process using the degradation of Acid Blue dye experiments. The reactor used

was a Continuous Stir Tank Reactor comprising of a closed pyrex reactor with an outer diameter of 42.0 mm and a height of 210 mm and thickness 4 mm. 50 mL of the dye solution containing 5 mg/L of Acid Blue was added to a 100 mL beaker and set up on a magnetic stirrer. 50 mg of the catalyst (ZnO-S.S.) was added to the reactor. The pH of the aqueous dye solution was kept at a pH of 7.3 during the reaction using a HANNA 4222 pH meter. The suspension was stirred by using a magnetic stirrer at 650 rpm at ambient temperature for 30 minutes in the dark, after which 5 mL of the suspension was withdrawn to analyse the equilibrium concentration of dye in the solution using a JENWAY 6705 Ultra violet-Visible Spectrophotometer. The mixture was then exposed to UV light and visible light. At selected time intervals of approximately 30 minutes over a typical 2 hours reaction time, 5 mL of the suspension was withdrawn with a syringe and filtered using a 0.45 µm PTFE membrane syringe filter (Acrodisc CR13 mm) and then taken for analysis using JENWAY 6705 Ultra violet-Visible Spectrophotometer. This procedure was repeated by varying concentration of the dye (10 mg/L and 15 mg/L) and varying catalyst dosage (100 mg and 150 mg) respectively.

The percentage of the Acid Blue degraded by the catalyst was calculated using the equation below:

$$\% \text{ Degradation} = \frac{C_o - C_e}{C_o} \cdot 100 \quad (1)$$

where C_o is the initial concentration of the Acid Blue before degradation, C_e is the equilibrium concentration (final concentration) of the dye after degradation.

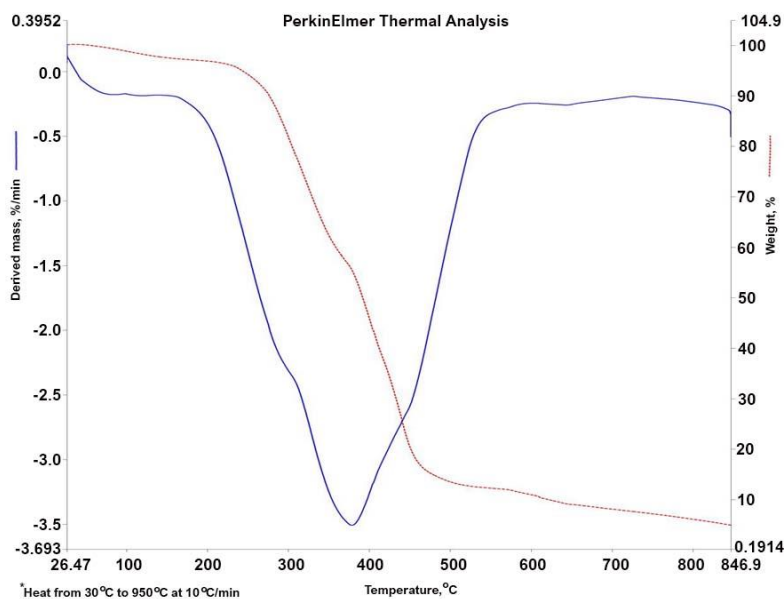


Figure 4. TGA- DTA of ZnO-S.S. nanoparticles

TGA reveals the thermal stability and percentage weight loss of the ZnO nanoparticle. There was 2% loss of weight as the temperature increased from 50 °C to 100 °C most likely due to loss of water of crystallization (moisture content). The sample also demonstrated thermal stability as the temperature increased from 100 °C to 250 °C. This is most possibly due to the loss of organic volatile matter during heating. As temperature increases from 250 °C to 460 °C, there was a significant weight loss of approximately 88% likely due to decomposition of the oxygen in the nanoparticles that might lead to the collapse of the spherical matrix. High thermal stability was obtained as temperature increases from 600 °C

RESULTS AND DISCUSSIONS

Characterization of ZnO-Senna Siamea Nanoparticles

Figure 3 represents image of the Transmission emission microscope analysis (TEM) analysis that gives further insight into some noteworthy details of the formed particles. It indicates that ZnO-S.S. nanoparticles are small spherical particles which conform to the uniform spherical shape revealed in the SEM analysis. The result was consistent with the previously reported study of change in the morphology of ZnO nanoparticles upon changing the reactant concentration by Borghei and Taleshi (2012).

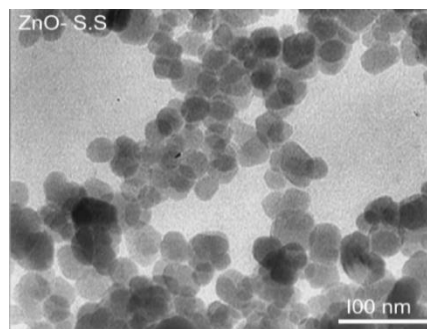


Figure 3. Transmission electron microscope of ZnO-S.S. nanoparticles (100 nm)

Figure 4 unveils the TGA- DTA of ZnO-S.S., it measures the mass of a sample as it is submitted to a selected temperature program in a defined atmosphere.

to 846.9 °C with an insignificant weight loss in contrast to the improved thermal constancy recorded for ZnO Passiflora foetida nanostructure after 400 °C (Khan et al., 2021). The weight of residue is about 5% while the sharp peak as temperature increases from 480 °C to 490 °C shows that the reaction is endothermic and occurred rapidly.

The Scanning electron microscope (SEM) analysis of ZnO-S.S. displayed in Figure 5, like the TEM also confirms that the nanoparticles are spherical in shape and uniformly distributed. This is consistent with previously reported study of Sayilkan and Emre (2016). SEM is a surface imaging method conducted to unveil surface morphology (Zhang, 2016).

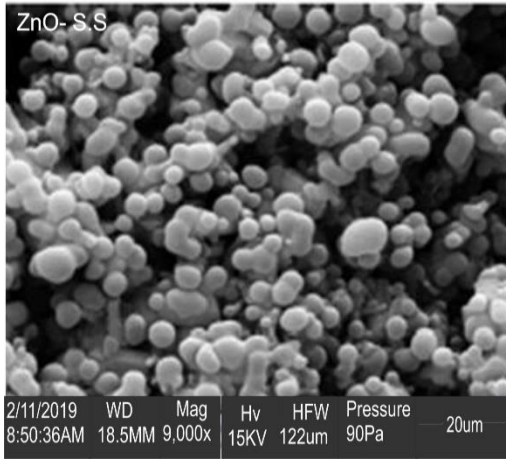


Figure 5. Scanning Electron Microscope of ZnO-S.S. nanoparticles ($\times 9000$)

To determine the elemental composition, atomic weight percentage and purity of the ZnO-S.S., The Energy dispersive X-ray (EDX) analysis of the synthesized ZnO-S.S. nanoparticles displayed in Figure 6 reveals the elemental composition and atomic weight percentage as C (4.8%), O (11%), S (6%) and Zn (78.2%) evidenced with a high peaks of Zn and O indicating the formation of ZnO nanoparticles while low peaks implies other components (C and S) or impurities present. Thereby, verifying the purity of ZnO nanoparticles. Similar result was obtained by Rajeshkumar et al. (2018) where they synthesized a pure form of nanoparticle clearly depicted through EDX imaging.

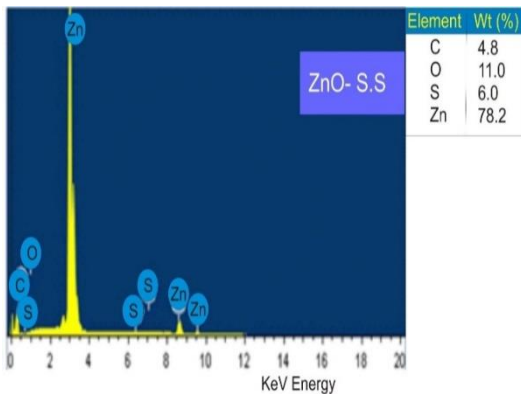


Figure 6. Elemental composition of ZnO-S.S. nanoparticles (EDX)

Photocatalytic degradation of Acid Blue Dye solution under visible irradiation

The percentage degradation of 5 mg/L Acid Blue Dye by means of visible light alongside 50 mg, 100 mg, and 150 mg ZnO-S.S. presented in Figure 6 followed the same pattern of increase with time. Evidently, the chart shows the 100 mg and 150 mg doses of ZnO-S.S. have the best percentage degradation of Acid Blue Dye by 97% at 150 mins. Even though initial increase in the dosage of the catalyst from 100 mg to 150 mg leads to turgidity hence reduces the efficiency of the initial degradation of the dye pollutant. This removal is comparable to the 97% efficiency of the degradation of Congo red dye within 2 hours at pH = 8 ZnO rod nanoparticle (Molahasani, 2019).

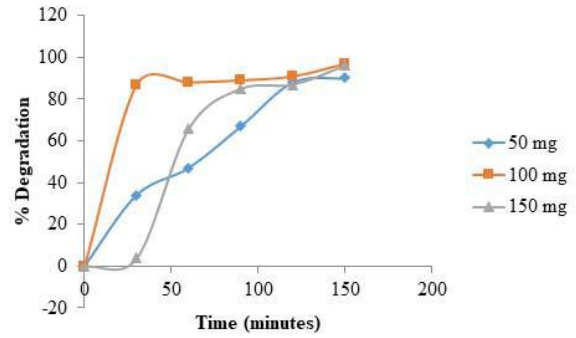


Figure 6. Effect of catalyst dosage (concentration = 5 mg/L, pH = 7.3)

In the degradation of 10 mg/L of the dye with 50 mg, 100 mg and 150 mg dose of ZnO-S.S., removal increases with time as demonstrated in Figure 7, the best dye removal efficiency of 99% was record at 150mins using 150 mg ZnO-S.S. This was quite greater than the 84% highest removal efficiency of acid blue 29 dyes on utilization of CdS-TiO₂ nanocomposites catalyst over a period of 90 minutes by visible light (Qutub et al., 2022). Therefore very clearly, this also implies that the 150 mg of ZnO-S.S. nanoparticles gave better removal efficiency than the other two doses of 50 mg and 100 mg respectively. The percentage degradation increased with increase dosage which could be due to availability of bonding sites in the solution (Mashael & Murefah, 2018).

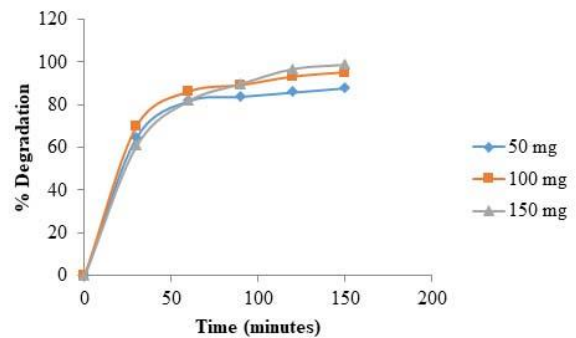


Figure 7. Effect of catalyst dosage (concentration = 10 mg/L, pH = 7.3) using

Figure 8 also shows similar trend with 97% as the highest dye percentage removal efficiency at 150 mins using 150 mg of ZnO-S.S. This is comparable with the 97% removal efficiency of acid blue 113 dye by ZnS/TiO₂ nanocomposite at the optimum condition of 0.5 g dosage and a pH of 6.2 (Almhana et al., 2022). The concentration of dye degraded increased as dosage decreases and this could be due to availability of saturated bonded sites in the solution. The observation follows Beer-Lambert law, wherein the increase in the initial dye concentration decreases the path length of the photons entering the solution, resulting in lowering the photon on the catalyst particles, which causes the photo-degradation rate to be lower (Mashael & Murefah, 2018).

Photocatalytic Degradation Kinetics of Acid Blue Dye Solution

In order to have a comprehensive understanding of the degradation process, Kinetic studies were carried out for the photocatalytic degradation of acid blue dye with time (30-mins interval) for 50 mg, 100 mg and 150 mg doses of ZnO-S.S. catalyst in the presence of visible light.

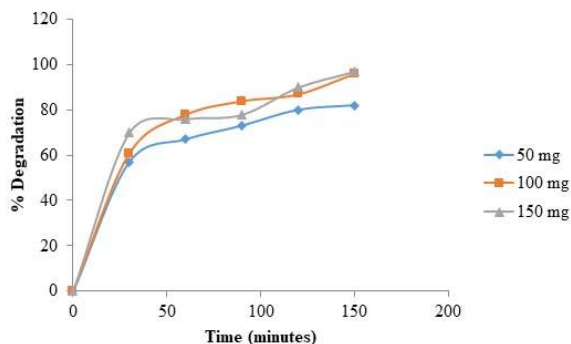


Figure 8. Effect of catalyst dosage (concentration = 15 mg/L, pH = 7.3)

The variations in concentration due to degradations were fitted into pseudo first order and second order kinetic models respectively. The kinetic data generated from the various models are presented in Table 1.

Table 1. Kinetic parameters for photocatalytic degradation of Acid Blue Dye solution

Dye concentration (mg/L)	First order	Second order
5	$R^2 = 0.8748$ $k_1 = 0.0174 \text{ (min}^{-1}\text{)}$ $Q_m = 5.3832 \text{ (mg/g)}$	$R^2 = 0.7693$ $k_2 = 0.1072 \text{ (g/mg/min)}$ $Q_m = 0.1907 \text{ (mg/g)}$
10	$R^2 = 0.9523$ $k_1 = 0.0198 \text{ (min}^{-1}\text{)}$ $Q_m = 6.8090 \text{ (mg/g)}$	$R^2 = 0.8295$ $k_2 = 0.1233 \text{ (g/mg/min)}$ $Q_m = 0.4056 \text{ (mg/g)}$
15	$R^2 = 0.8967$ $k_1 = 0.0149 \text{ (min}^{-1}\text{)}$ $Q_m = 9.9342 \text{ (mg/g)}$	$R^2 = 0.7821$ $k_2 = 0.1385 \text{ (g/mg/min)}$ $Q_m = 0.4836 \text{ (mg/g)}$

Based on the highest value of regression coefficients (R^2) obtained (William et al., 2019; Yerima et al., 2023), the photocatalytic degradation of 5 mg/L, 10mg/L and 15 mg/L of acid blue dye solution best fits the pseudo first order kinetics $R^2 = 0.8748$ to $R^2 = 0.9523$ and at the rate constant of $k_1 = 0.0174 \text{ (min}^{-1}\text{)}$ to $k_1 = 0.0198 \text{ (min}^{-1}\text{)}$ respectively. First order kinetics implies that the rate of acid blue dye degradation in the waste water was proportional to the concentrations of the ZnO-S.S. catalyst (McMartin et al., 2012).

CONCLUSION

This study confirms the photocatalytic degradation of Acid Blue dye by ZnO-S.S. nano-particle synthesized from *Senna siamea* flower extract as a useful and economic catalyst for waste water treatment with 97% to 99% efficiency. The study reveals that the synthesized ZnO-S.S. nano-particle exhibited appreciable purity and good photocatalytic properties suitable for an enhanced degradation process of contaminants in waste water. The degradation trend of acid blue dye contaminant increases proportionately with increase in catalyst dose in the case of 10 mg/L and 15 mg/L concentrations. The optimum dose of ZnO-S.S. nano-particle for degradation of the acid blue dye contaminant was 150 mg with removal efficiencies of 99% (150 minutes) and 97% (150 minutes) for 10 mg/L and 15 mg/L concentrations respectively following the pseudo first order.

Author's statements

Acknowledgments

The authors acknowledge and thank the Head of Chemistry Department, Ahmadu Bello University Zaria for allowing us use facilities in the Chemistry laboratory during this study.

Contributions

The authors declare that they have made equal contributions to the current research, namely: Conceptualization, Formal Analysis, Investigation, Methodology, Validation, Visualization, Writing – original draft, Writing – review & editing were performed by B.N.H. and G.G.Y.

Declaration of conflicting interest

The authors declare no competing interests.

Financial interests

The authors declare they have no financial interests.

Funding

Not applicable.

Data availability statement

No data were used for the current study.

AI Disclosure

The author declares that generative AI was not used to assist in writing this manuscript.

Ethical approval declarations

Not applicable.

Additional information

Publisher's note

Publisher remains neutral with regard to jurisdictional claims in published maps and institutional affiliations.

REFERENCES

- Agarwal, H., Menon, S., Kumar, S. V., & Rajeshkumar, S. (2018). Mechanistic study on antibacterial action of zinc oxide nanoparticles synthesized using green route. *Chemico-Biological Interactions*, 286, 60–70. <https://doi.org/10.1016/j.cbi.2018.03.008>.
- Ahmed, S., Chaudhry, S. A., & Ikram, S. (2017). A review on biogenic synthesis of ZnO nanoparticles using plant extracts and microbes: a prospect towards green chemistry. *Journal of Photochemistry and Photobiology B: Biology*, 166, 272–284. <https://doi.org/10.1016/j.jphotobiol.2016.12.011>.
- Almhana, N. M., Al-Najjar, S. Z., Naser, Z. A., Al-Sharif, Z. T., & Nail, T. H. (2022). Photocatalytic degradation of textile dye from wastewater by using ZnS/TiO₂ nanocomposites material. *Egyptian Journal of Chemistry*, 65(131), 481–488. <https://doi.org/10.21608/EJCHEM.2022.125852.5588>.
- Alshabanat, M. N., & AL-Anazy, M. M. (2018). An experimental study of photocatalytic degradation of Congo red using polymer nanocomposite films. *Journal of Chemistry*, 2018, 1–8. <https://doi.org/10.1155/2018/9651850>.
- Ansari, M. O., Khan, M. M., Ansari, S. A., & Cho, M. H. (2015). Electrically conductive polyaniline sensitized defective-TiO₂ for improved visible light photocatalytic and photoelectrochemical performance: A synergistic effect. *New Journal of Chemistry*, 39(11), 8381–8388. <https://doi.org/10.1039/C5NJ01127B>.

- Awwad, A. M., Albiss, B. A., & Salem, N. M. (2015). Antibacterial activity of synthesized copper oxide nanoparticles using *Malva sylvestris* leaf extract. *SMU Medical Journal*, 91–101.
- Azizi, S., Mahdavi Shahri, M., & Mohamad, R. (2017). Green synthesis of zinc oxide nanoparticles for enhanced adsorption of lead ions from aqueous solutions: equilibrium, kinetic and thermodynamic studies. *Molecules*, 22(6), 831. <https://doi.org/10.3390/molecules22060831>.
- Donkadokula, N. Y., Kola, A. K., Naz, I., & Saroj, D. (2020). A review on advanced physico-chemical and biological textile dye wastewater treatment techniques. *Reviews in Environmental Science and Bio/Technology*, 19, 543–560. <https://doi.org/10.1007/s11157-020-09543-z>.
- Gupta, V. K., Ali, I., Saleh, T. A., Nayak, A., & Agarwal, S. (2012). Chemical treatment technologies for waste-water recycling – an overview. *Rsc Advances*, 2(16), 6380–6388. <https://doi.org/10.1039/C2RA20340E>.
- Inyinbor Adejumo, A., Adebisin Babatunde, O., Oluyori Abimbola, P., Adelani Akande Tabitha, A., Dada Adewumi, O., & Oreofe Toyin, A. (2018). Water pollution: effects, prevention, and climatic impact. *Water Challenges of an Urbanizing World*, 33, 33–47. <http://dx.doi.org/10.5772/intechopen.72018>.
- Jayachandran, A., Aswathy, T. R., & Nair, A. S. (2021). Green synthesis and characterization of zinc oxide nanoparticles using *Cayratia pedata* leaf extract. *Biochemistry and Biophysics Reports*, 26, 100995. <https://doi.org/10.1016/j.bbrep.2021.100995>.
- Kajjumba, G. W., Emik, S., Öngen, A., Özcan, H. K., & Aydın, S. (2018). Modelling of adsorption kinetic processes—errors, theory and application. *Advanced Sorption Process Applications*, 1–19. <https://doi.org/10.5772/intechopen.80495>.
- Khan, M., Ware, P., & Shimpi, N. (2021). Synthesis of ZnO nanoparticles using peels of *Passiflora foetida* and study of its activity as an efficient catalyst for the degradation of hazardous organic dye. *SN Applied Sciences*, 3, 1–17. <https://doi.org/10.1007/s42452-021-04436-4>.
- Kpega, T. C., Habila, J. D., Okon, I. E., & Ekwumemgbo, P. A. (2023). Green synthesis and characterization of zinc oxide nanoparticles using *Corchorus olitorius* leaf extract. *Aceh International Journal of Science and Technology*, 12(3), 358–367. <https://doi.org/10.13170/aijst.12.3.34013>.
- McMartin, K. E., Sebastian, C. S., Dies, D., & Jacobsen, D. (2012). Kinetics and metabolism of fomepizole in healthy humans. *Clinical Toxicology*, 50(5), 375–383. <https://doi.org/10.3109/15563650.2012.683197>.
- Moghri Moazzen, M. A., Borghei, S. M., & Taleshi, F. (2013). Change in the morphology of ZnO nanoparticles upon changing the reactant concentration. *Applied Nanoscience*, 3, 295–302. <https://doi.org/10.1007/s13204-012-0147-z>.
- Molahasani, N. (2019). Photocatalytic degradation of Congo red by ZnO nanoparticles with different morphology. *Journal of Interfaces, Thin Films, and Low Dimensional Systems*, 3(1), 219–226. <https://doi.org/10.22051/jitl.2020.31515.1039>.
- Qutub, N., Singh, P., Sabir, S., Sagadevan, S., & Oh, W. C. (2022). Enhanced photocatalytic degradation of Acid Blue dye using CdS/TiO₂ nanocomposite. *Scientific Reports*, 12(1), 5759. <https://doi.org/10.1038/s41598-022-09479-0>.
- Rajeshkumar, S., Kumar, S. V., Ramaiah, A., Agarwal, H., Lakshmi, T., & Roopan, S. M. (2018). Biosynthesis of zinc oxide nanoparticles using *Mangifera indica* leaves and evaluation of their antioxidant and cytotoxic properties in lung cancer (A549) cells. *Enzyme and Microbial Technology*, 117, 91–95. <https://doi.org/10.1016/j.enzmictec.2018.06.009>.
- Rinde, E., & Troll, W. (1975). Metabolic reduction of benzidine azo dyes to benzidine in the rhesus monkey. *Journal of the National Cancer Institute*, 55(1), 181–182. <https://doi.org/10.1093/jnci/55.1.181>.
- Shah, M. P. (2014). Microbial degradation of acid blue dye by mixed consortium. *International Journal of Bioremediation & Biodegradation*, 2(3), 125–132. <https://doi.org/10.12691/ijebb-2-3-5>.
- Singh, P., Kim, Y. J., Zhang, D., & Yang, D. C. (2016). Biological synthesis of nanoparticles from plants and microorganisms. *Trends in Biotechnology*, 34(7), 588–599. <https://doi.org/10.1016/j.tibtech.2016.02.006>.
- Wang, C., Yediler, A., Lienert, D., Wang, Z., & Ketrup, A. (2002). Toxicity evaluation of reactive dyestuffs, auxiliaries and selected effluents in textile finishing industry to luminescent bacteria *Vibrio fischeri*. *Chemosphere*, 46(2), 339–344. [https://doi.org/10.1016/S0045-6535\(01\)00086-8](https://doi.org/10.1016/S0045-6535(01)00086-8).
- Yerima, E. A., & Johnson, S. N. Assessment of Nutrient Availability and Competition Between *Striga Hermonthica* and Maize Plant. *International Journal of Environmental Monitoring and Analysis*, 11(5), 106–113.
- Yerima, E. A., Kamba, E. A., Egah, G. O., Ma'aji, S. P., Ibrahim, I. A., & Zulkifli, S. (2022). Quality Index of Borehole Water in Marmara and New Site Communities of Wukari, Nigeria. *UMYU Scientifica*, 1(1), 114–121. <https://doi.org/10.56919/usc.1122.015>.
- Zhang, L., & Fang, M. (2010). Nanomaterials in pollution trace detection and environmental improvement. *Nano Today*, 5(2), 128–142. <https://doi.org/10.1016/j.nantod.2010.03.002>.